In vivo NMR study of yeast fermentative metabolism in the presence of ferric irons

Maso Ricci[1,2,*], Silvia Martini[1,2], Claudia Bonechi[1,2], Daniela Braconi[3], Annalisa Santucci[3] and Claudio Rossi[1,2]

[1]*Department of Pharmaceutical and Applied Chemistry, University of Siena, Via Aldo Moro, 2–53100 Siena, Italy*

[2]*Center for Colloid and Surface Science (CSGI), Via della Lastruccia 3, Sesto Fiorentino, FI, Italy*

[3]*Department of Molecular Biology, Università di Siena, Via Fiorentina, 1–53100 Siena, Italy*

**Corresponding author (Fax,+390577234177; Email, ricci2@unisi.it)*

Mathematical modelling analysis of experimental data, obtained with *in vivo* NMR spectroscopy and ^{13}C-labelled substrates, allowed us to describe how the fermentative metabolism in *Saccharomyces cerevisiae*, taken as eukaryotic cell model, is influenced by stress factors. Experiments on cellular cultures subject to increasing concentrations of ferric ions were conducted in order to study the effect of oxidative stress on the dynamics of the fermentative process. The developed mathematical model was able to simulate the cellular activity, the metabolic yield and the main metabolic fluxes occurring during fermentation and to describe how these are modulated by the presence of ferric ions.

[Ricci M, Martini S, Bonechi C, Braconi D, Santucci A and Rossi C 2011 *In vivo* NMR study of yeast fermentative metabolism in the presence of ferric irons. *J. Biosci.* **36** 97–103] **DOI** 10.1007/s12938-011-9003-7

1. Introduction

Iron is an essential element required by all eukaryotes and by a great majority of prokaryotes. The ability of iron to easily gain and lose electrons, transitioning between two valence states, has made it an essential component for a broad range of redox reactions. Iron can be very toxic to living organisms when present in excess, because it leads to an increased oxidative stress (Estruch 2000; Aisen *et al.* 2001; Costa and Moradas-Ferreira 2001; Peiter *et al.* 2005b). Changes in the ion levels of nutrient media alter the intracellular concentration of the ions themselves, thus provoking specific biochemical and physiological responses (Puig *et al.* 2005). Several studies have highlighted the stress effects of high iron concentration on the metabolic pathways, but only a few have considered this aspect of iron metabolism and regulation from a modellistic point of view (Gligic *et al.* 2003).

Saccharomyces cerevisiae represents an ideal model system to investigate the effects of environmental conditions on eukaryotic metabolic processes.

The literature provides a large number of studies that explain the processes taking place at the molecular level during the adaptive efforts of *S. cereviasiae* in response to external stimuli. Nevertheless, an approach to describe and understand the complex network of interactions among the different components of the system needs to be applied.

Mathematical modelling represents a fundamental tool to investigate and understand the kinetics of cell metabolism. Michaelis-Menten and exponential kinetics have played an essential role in the study of microorganism metabolism (Beechem 1992; Jacquez 1996), but they have failed to provide a reliable instrument for explaining the metabolic mechanisms that involve interactions between cells, precursors and products.

This article presents an approach that takes advantage of the combined use of *in vivo* ^{13}C NMR spectroscopy and mathematical modelling in order to investigate cellular metabolic dynamics. The use of ^{13}C-labelled substrates allows one to follow the entire process of substrate degradation and product formation *in vivo*, with no need of external samplings (den Hollander *et al.* 1979; Shulman *et al.*

Keywords. Ethanol yield; *in vivo* NMR; iron metabolism; mathematical modelling; oxidative stress; *Saccharomyces cerevisiae*

1979; Shulman 1983). In particular, our modelling approach takes into account the effects of exogenous stress factors that influence the metabolic behaviour of microorganisms. We clearly have already shown that this approach provides the biological information indicating the cell response to strong stress factors, such as the presence of exogenous ethanol during the sugar fermentation by cultures of *S. cerevisiae* (Martini *et al.* 2004, 2005; Ricci *et al.* 2004)

We present here a study on the effects of increasing concentrations of ferric ions (as ferric chloride) on the fermentation metabolism in *S. cerevisiae*. The developed model allows the interpretation of the cell response in terms of a reduced metabolic activity, at the beginning of fermentation, as a function of ferric iron concentration.

2. Materials and methods

All high-purity reagents were purchased from Sigma-Aldrich (Milano, Italy), Merck Eurolab (Milano, Italy), Carlo Erba (Rodano, MI, Italy) and Serva (Heidelberg, Germany). All the water used was Milli-Q quality (Millipore, Bedford, USA). 1-^{13}C glucose was from Cambridge Isotope Laboratories (Andover, MA, USA).

2.1 *Yeast strain and culture conditions*

Saccharomyces cerevisiae K310 strain was isolated from naturally fermenting must during vinification of a high-quality wine, in the geographical area of 'Brunello di Montalcino', and is well-characterized physiologically for its protein repertoire and stress response (Trabalzini *et al.* 2003).

A pure culture was grown in yeast peptone dextrose (YPD) at 30°C with rotary shaking (120 rpm) for 10 h. An aliquot of the saturated culture was inoculated in YPD, adjusted to a final pH of 4.5 by adding 0.2 M citrate-phosphate buffer and containing 100 g/l unlabelled glucose in order to obtain an initial cell concentration of 1×10^4 cells/ml. The cell suspension was then incubated at 28°C without shaking, in order to allow semi-anaerobic growth. Samples were collected at different times during the growth. At each sampling, the pH of the cell suspension was checked and growth was monitored by measuring the absorbance of the culture at 660 nm.

2.2 *Sample preparation for in vivo ^{13}C NMR experiments*

Saccharomyces cerevisiae cell suspensions at 1×10^6 cells/ml, indicating an early log phase of growth, were centrifuged for 5 min at room temperature and 3000*g* in a Beckman centrifuge model J2-21 equipped with a JA10 rotor. The supernatant was discarded and the pellets were resuspended in 0.5 ml of the same medium (YPD) containing 100 g/l of (1-^{13}C)- glucose, and transferred to a 5 mm NMR tube. Also, 20% (v/v) of D_2O was added to provide a lock signal.

Three sets of experiments were conducted during which the same batch conditions were used except for the ferric chloride concentration, which was 0, 20 and 40 mM.

2.3 *NMR measurements*

^{13}C NMR spectra were collected with a Varian VXR 300 spectrometer operating at 300 and 75 MHz for proton and carbon nuclei, respectively. Carbon spectra were recorded under continuous broadband decoupling conditions. An array in d1 parameter of the pulse sequence was used, so that carbon spectra were recorded at time intervals of 6 min. During the experiments the NMR probe was thermostated at 30°C. The substrate and the end-product concentrations were calculated from the area of NMR peaks by means of an appropriate calibration.

The total ethanol concentration was estimated by quantitative ^{1}H NMR measurements, using as an internal standard 3-tetramethylsylil-2,2,3,3-tetradeutero-proprionic acid, Na salt (TSP) and a calibration curve built with standard ethanol solutions in YPD.

A parallel growth was carried out during the yeast growth under the NMR monitoring. Samples were collected at time 0 and after 12, 16, 19, 22, 27, 36, 44, 50 and 62 h. At each sampling the pH of the cell suspension was checked and growth was monitored by measuring the absorbance of the culture at 660 nm. The pH (4.5) never changed during cell growth, as already reported (Peiter *et al.* 2005a).

2.4 *Mathematical modelling*

The model parameter values were estimated by the nonlinear regression analysis using the Marquardt–Levemberger method implemented in the MLAB software (Knott and Kerner 2004).

3. Results and discussion

Figure 1 shows the metabolic pathway of glucose-to-ethanol fermentation by *S. cerevisiae*.

Owing to the high initial concentration of glucose (100 g/l) used *in vivo* NMR experiments, we assumed that the main metabolic pathway for the degradation of this substrate in *S. cerervisiae* K310 was fermentation. In fact, when yeast grows in the presence of high glucose concentrations, the repression exerted by sugar on the other metabolic pathways makes fermentation the main degradation pathway (Crabtree effect) (Fiechter *et al.* 1981; De Deken 1996). Thus, we considered glucose as the unique carbon source, and ethanol as the main end product of the fermentative process.

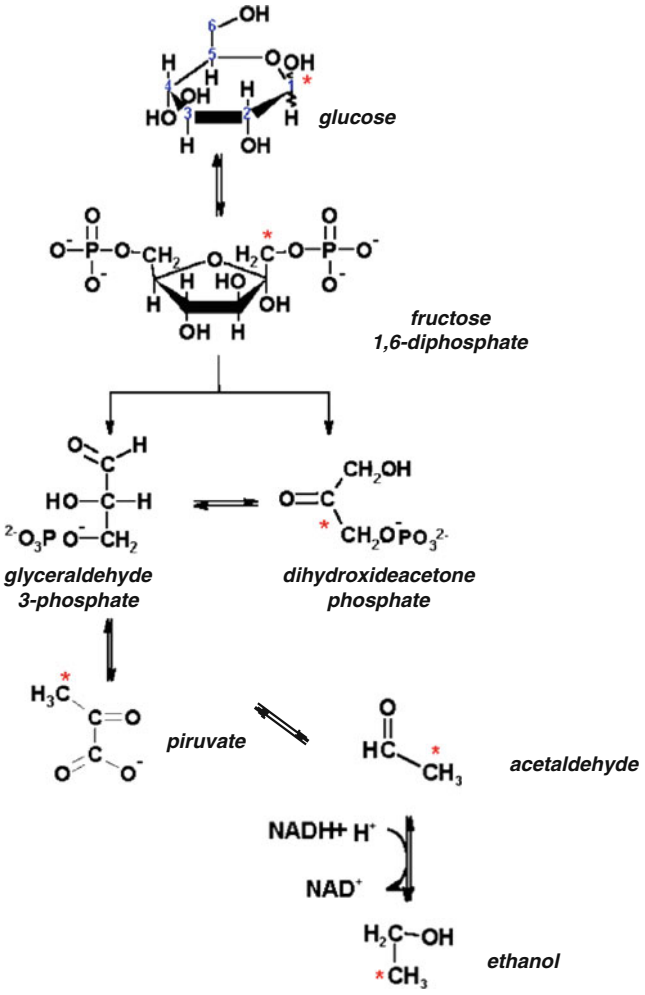

Figure 1. Metabolic pathway of glucose-to-ethanol fermentation by *S. cerevisiae*. The asterisks refer to the position of the ^{13}C label.

Three sets of experimental data were collected using NMR spectroscopy during the fermentation process of 100 g/l of (1-^{13}C)-glucose without added iron and in the presence of $FeCl_3$ 20 and 40 mM, respectively, in order to study the effect of an iron-replete medium on the fermentative metabolism of the wild-type yeast *S. cerevisiae* K310.

Figure 2 shows the carbon-13 spectra acquired at various sampling times. The integrated peaks area of ^{13}C NMR spectra provided the experimental data of glucose and ethanol concentrations in relation to time.

Data (refer figure 5 for experimental results) show that the dynamics of glucose degradation and ethanol production were slightly decreased by the presence of ferric chloride, while both the ethanol yield and the time of fermentation remained almost unchanged. Indeed, close to the end of fermentation the error bars somewhat overlap. This indicates that the final ethanol yield was not significantly affected by iron, whereas glucose concentration approached zero in about 40 h in all the three experiments.

The theoretical *ethanol yield* can be calculated by considering the stoichiometry of the bioconversion of glucose to ethanol in the fermentative pathway:

$$\mathbf{C_6H_{12}O_6} + 2\,\mathrm{Pi} + 2\,\mathrm{ADP} + 2\mathrm{H}^+ \rightarrow 2\,\mathbf{C_2H_5OH} + 2\,\mathrm{CO_2} + 2\,\mathrm{ATP} + 2\mathrm{H_2O}. \quad (1)$$

The ethanol yield is equal to the ratio of ethanol and glucose concentrations (expressed in g/l), and its maximum theoretical value (ThY) equals 0.51, assuming that all the glucose is converted to ethanol.

We consider the fermentative route as the main catabolic pathway for glucose in our experimental conditions, although glucose enters in many metabolic pathways (and is converted, for example, into ethanol, CO_2, glycerol and biomass).

The experimental yield can be derived from experimental data by plotting the ethanol time course vs. the metabolized glucose time course (figure 3). A linear dependence is evident and the slope of each line, calculated by linear regression, represents the experimental metabolic yield (EMY) (table 1).

It can be noticed that the experimental ethanol yield presents similar values in all of the three experiments. Therefore, taking into consideration the error on the final ethanol determination (table 1), we can affirm that metabolic ethanol yield is not significantly affected by ferric chloride.

3.1 *Mathematical model*

The experimental evidences obtained from *in vivo* NMR data represented the basis for developing a mathematical model (Curto *et al.* 1995; Goel *et al.* 2006).

The model is composed of a few variables: glucose concentration [*G*], the produced ethanol concentration [*E*] and cellular activity [*C*]. The latter is an adimensional index related to the number of active cells and modulated by the inhibition processes due to the presence of endogenous and exogenous stress factors (i.e. ethanol and Fe^{III} ions).

We have considered the overall fermentation process described by equation 1 in order to describe the metabolization of glucose.

Instead of taking into account the totality of the metabolic reactions involved in the fermentative pathway, we considered all the metabolic steps in between as a kind of black box. Because the aim of our model is a holistic description of the cellular system as a whole, this model focused on the overall fermentation process (Warwick *et al.* 2007).

We assumed that the dynamics of glucose metabolization results from an autocatalytic process depending on both the

concentration of the available carbon source (glucose) and the cellular activity. The presence of the sugar promotes an energy flow to the active cells, which allows the cell culture to grow:

$$\frac{d[G]}{dt} = -k_D[G][C], \tag{2}$$

where k_D is the rate constant for the glucose consumption.

Given that glucose enters different metabolic pathways depending on the condition of the system, the kinetic parameter k_D incorporates several kinetic constants of all the metabolic pathways involving the consumption of glucose. According to this, equation 1 describes the dynamics of glucose metabolization, which is the sum of several parallel reactions (Klipp *et al.* 2005).

We have considered the bioconversion of glucose into ethanol, as described by equation 1, in order to derive the kinetic law of endogenous ethanol formation; this implies that, when molar concentration is used, the following equation can be applied:

$$\frac{d[E]}{dt} = -2\frac{d[G]}{dt}. \tag{3}$$

Therefore, by equation 2, the dynamics of production of ethanol will be:

$$\frac{d[E]}{dt} = 2k_D[G][C]. \tag{4}$$

The coefficient in equation 4 is the maximum yield (Y_M) when using molar concentration and it corresponds to the maximum theoretical yield expressed in g/l (ThY=0.51). This value implies a theoretical condition in which the total amount of glucose is metabolized to ethanol in the fermentative pathway. If $Y_M<2$, then a percentage of glucose would be metabolized in other metabolic pathways.

Indeed, equation 4 could be written in a more general form:

$$\frac{d[E]}{dt} = Rk_D[G][C], \tag{5}$$

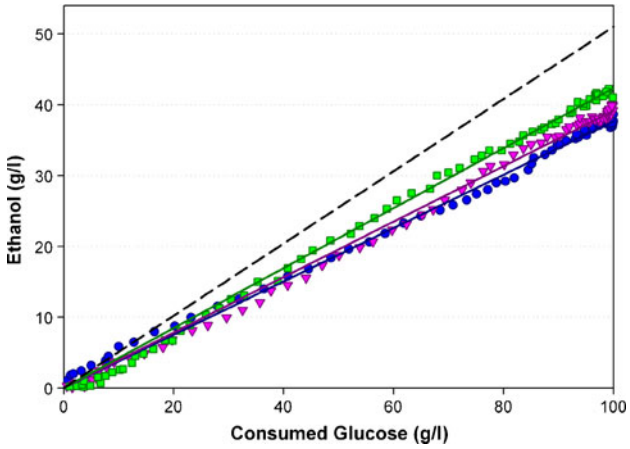

Figure 3. Endogenous ethanol vs. metabolised glucose during glucose fermentation in *S. cerevisiae* K310 in the presence of $FeCl_3$: blue (●)=0 mM, pink (▼)=20 mM and green (■) =40 mM. The slope of each line was calculated by linear regression. The theoretical maximum yield (0.511) is also reported (*dashed line*).

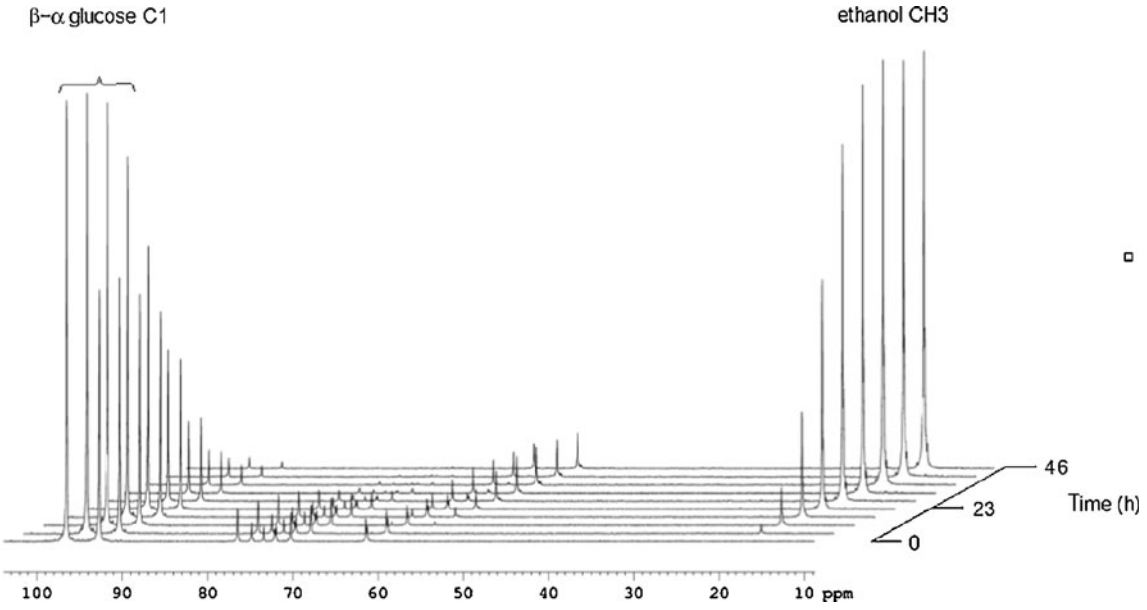

Figure 2. Representative ^{13}C NMR spectra obtained during glucose fermentation by *S. cerevisiae*.

Table 1. Final ethanol concentrations determined by a calibration curve using quantitative ^{1}H NMR measurements and experimental metabolic yield (EMY) calculated as the slopes of the lines shown in figure 4

$FeCl_3$ (mM)	Final EtOH (g/l)	Standard Deviation	EMY (y=EMY x)	Standard Deviation
0	39	±1.96	0.376	$\pm 3\times10^{-4}$
20	40	±1.96	0.391	$\pm 4\times10^{-4}$
40	41	±1.96	0.423	$\pm 4\times10^{-4}$

where R is a general parameter expressing the fraction of glucose metabolized to ethanol, i.e. the ethanol yield.

Equation 6 describes the time course of cellular activity:

$$\frac{d[C]}{dt} = \underbrace{k_A[G][C]}_{A} - \underbrace{k_I[E][C]}_{B}, \quad (6)$$

where k_A and k_I are the kinetic constants associated to glucose activation and ethanol inhibition, respectively.

Equation 6 is based on the general form of logistic growth of a population. In agreement with the Monod equation (Monod 1949), the first term (A) of the equation expresses the growth of [C] as a function of glucose concentration. In its second term (B), the equation takes into account the inhibition due to the endogenous ethanol, which, being a well-known stress factor on yeast metabolism, provokes a decrease in the cellular activity (Martini *et al.* 2004, 2005; Ricci *et al.* 2004).

We could consider different stress factors depending on the system under consideration. The values of [C] at the beginning of fermentation $[C]_{t=0}$ is assumed to be 1, but this value tends to decrease in the presence of stress agents since the beginning of the fermentation. Therefore, in order to take into account the modulation of [C] due to increasing concentrations of ferric chloride, we need to consider a new element within the system itself, i.e. a further metabolic pathway activated only in the presence of $FeCl_3$ and capable of decreasing the value of $[C]_{t=0}$. This new metabolic pathway was simulated by the introduction in the model equation 7 whose trend, reported in figure 4, is sigmoidal and decreases with increasing iron concentration. This is in agreement with the fact that in the experimental data the dynamics in the first stages of fermentation become slower with increasing iron concentration. $[C]_{t=0}$ is thus described by the following equation:

$$[C]_{t=0} = [C_0]\frac{1}{1 + h[Fe^{3+}]^2}, \quad (7)$$

where h is a parameter that controls the initial concentration of active cells $[C]_{t=0}$ when $FeCl_3$ is added to the fermentation medium.

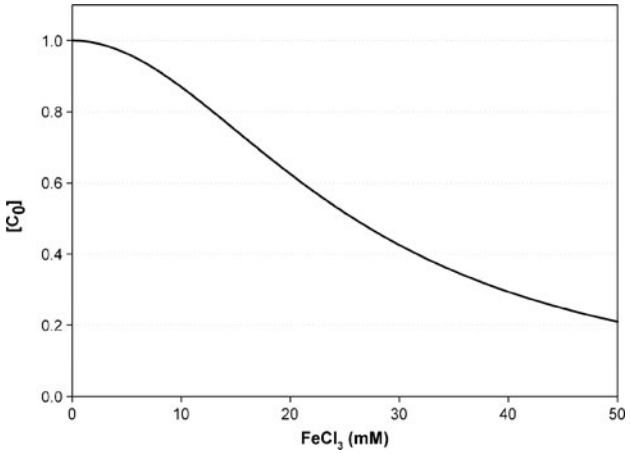

Figure 4. Simulation of cellular activity at time=0 [C_0] vs. $FeCl_3$ concentration.

3.2 *Validation of the model*

The validity of the model has been checked against experimental data. The values of the kinetic constants and the parameters in each equation were optimised by a nonlinear least square estimation technique, implemented in MLAB (Knott and Kerner 2004) (table 2). For the fitting, the three sets of experimental data were used simultaneously, as the values of parameters k_D, k_A, k_I and h were forced to remain the same in each data set. The R parameter (one for each data set) represents the experimental metabolic yields in ethanol (table 1) and was not included in the fitting procedure.

The agreement between experimental data and the model was excellent, as highlighted by the simulation of glucose degradation and ethanol formation calculated by the model (figure 5) and from the value of the correlation coefficient R^2=0.997.

Some interesting conclusions can be deduced by analysing the values of the constants calculated from the model (table 2). In particular, the slower fermentation rate observed in the presence of Fe^{III} is only due to a decreasing of the cellular activity at the beginning of the fermentation. In fact, experimental data showed that the yeast cells completely degraded the substrate even in the presence of the stress

Table 2. Estimated values and coefficient of variation (CV%) of the kinetics parameters

Parameters	Units	Value	CV%
k_D	s^{-1}	2.97×10^{-6}	0.8
k_A	$l\ g^{-1}\ s^{-1}$	5.97×10^{-7}	0.5
k_I	$l\ g^{-1}\ s^{-1}$	1.93×10^{-7}	4.4
h	$l^2\ mmol^{-2}$	1.11×10^{-3}	1.0

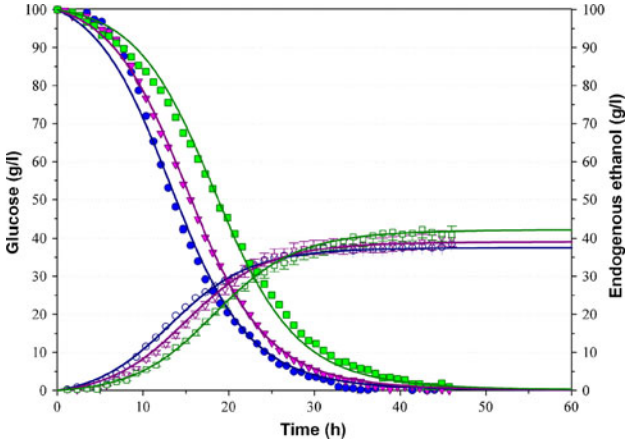

Figure 5. Experimental (symbols) and simulated (continuous line) time course of glucose and ethanol during glucose fermentation in *S. cerevisiae* K310 in the presence of $FeCl_3$. For the symbols refer to figure 2.

source, implying that the concentration of active cells represents the sole variable able to affect the rate of glucose degradation.

Figure 6 shows the simulated behaviour of cellular activity in relation to time calculated using equation 6 for each experiment. This is the result of two contributions: at the beginning of fermentation the high glucose concentration induces the increase of cellular activity with a rate equal to the activation parameter k_A, while an opposite effect is caused by the produced ethanol, which inhibits the fermentation process and thus decreases the cellular activity with a rate equal to the inhibition parameter k_I. As expected, k_A assumes higher values than k_I, so that the ability of glucose to promote the fermentation process is greater than the feedback inhibition due to the presence of ethanol, thus causing this curve to be non-symmetrical in respect to time.

The simulated behaviour of cellular activity vs. time, reported in figures 6 and 7, allows us to deduce that the effect of ferric iron concentrations ranging from 0 mM to 40 mM is temporary: during the first stages of the fermentative process (until about 30 h), cellular activity decreases with increasing iron concentration, indicating a stress effect. From about 30 h until the end of fermentation, cellular activity reaches the values assumed in the absence of exogenous stress factor (i.e. ferric iron). This trend is in agreement with the slowing down of glucose degradation dynamics in the experimental data and with similar ethanol yield values calculated for the three experiments.

The combined use of mathematical modelling and *in vivo* ^{13}C NMR spectroscopy proved to be a powerful tool for *in vivo* investigation of metabolism and its modulation in response to increasing ferric chloride concentration in the fermentation medium of a wild-type strain of *S. cerevisiae*.

The schematization obtainable by the developed compartmental model highlights the principal biochemical processes of glucose metabolism in yeast, i.e. the glucose metabolization and products formation and their modulation as a function of the ferric iron concentration.

Further, in particular, the model highlights that the presence of ferric ions in the range 0–40 mM causes the modulation of the dynamics of the fermentative metabolism in *S. cerevisiae* K310 during the first stages but does not affect in a significant manner the final ethanol yield. This is explained in terms of a reduced metabolic activity at the beginning of fermentation that is a function of ferric iron concentration.

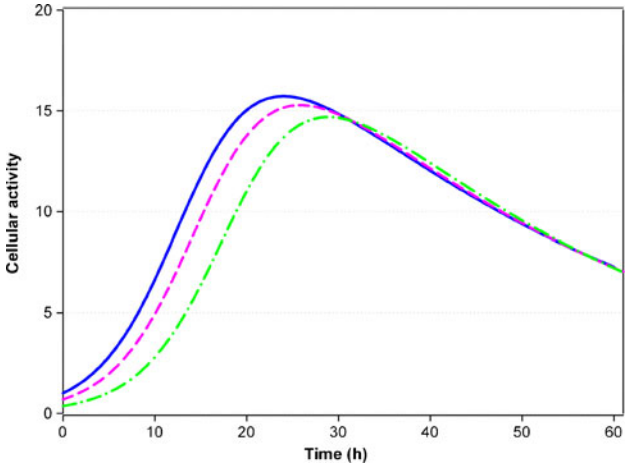

Figure 6. Cellular activity curves simulated by the model (equation 15): in the absence of added $FeCl_3$ (continuous line), with 20 and 40 mM of $FeCl_3$ (dashed and dash-dotted lines, respectively).

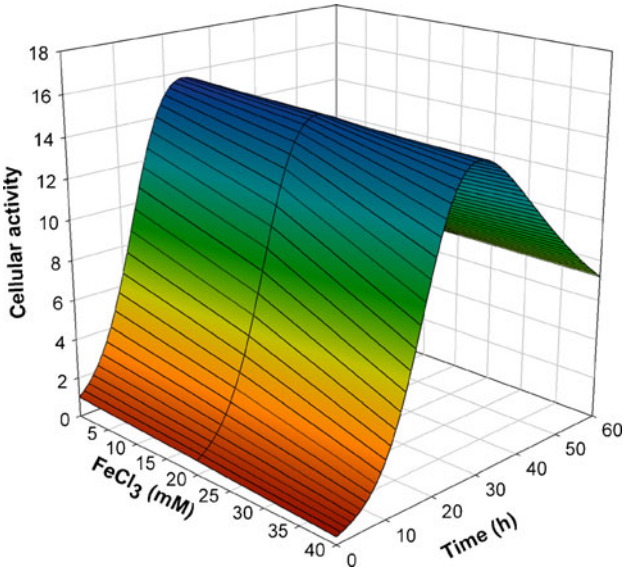

Figure 7. 3D surface of simulated cellular activity vs. time and $FeCl_3$ concentration.

Acknowledgements

This work was supported by MIUR Fondo per gli Investimenti della Ricerca di Base (FIRB), n. RBAU01JE9A, and Fondazione Monte dei Paschi di Siena Grants 2004 and 2005.

References

Aisen P, Enns C and Wessling-Resnick M 2001 Chemistry and biology of eukaryotic iron metabolism. *Int. J. Biochem. Cell Biol.* **33** 940–995

Beechem M 1992 Global analysis of Biochemical and biophysical data. *Methods Enzymol.* **210** 37–54

Costa V and Moradas-Ferreira P 2001 Oxidative stress and signal transduction in *Saccharomyces cerevisiae*: insights into ageing, apoptosis and diseases. *Mol. Aspect. Med.* **22** 217–246

Curto R, Sorribas A and Cascante M 1995 Theory and metabolic control analysis: model definition and momenclature. *Math. Biosci.* **130** 25–50

De Deken RH 1996 The Crabtree effect: a regulatory system in yeast. *J. Gen. Microbiol.* **44** 149–156

den Hollander JA, Brown TR, Ugurbil K and Shulman RG 1979 ^{13}C nuclear magnetic resonance studies of anaerobic glycolysis in suspensions of yeast cells. *Proc. Natl. Acad. Sci. USA* **205** 6096–6100

Estruch F 2000 Stress-controlled transcription factors, stress-induced genes and stress tolerance in budding yeast. *FEMS Microbiol. Rev.* **24** 469–486

Fiechter A, Fuhrmann GF and Kappeli O 1981 Regulation of glucose metabolism in growing yeast cells. *Adv. Microb. Physiol.* **22** 123–183

Gligic L, Vujovic N, Stevovic B and Manic J 2003 Optimal conditions for accumulation of bioavailable iron in *Saccharomyce cerevisiae* cells. *Boll. Chim. Farm.* **142** 330–332

Goel G, Chou IC and Voit EO 2006 Biological systems modelling and analysis: a biomolecular technique of the twenty-first century. *J. Biomol. Tech.* **17** 252–269

Jacquez JA 1996 *Compartmental analysis in biology and medicine*. (Ann Arbor: BioMedware) p. 514

Klipp E, Nordlander B, Kruger R, Gennemark P and Hohmann S 2005 Integrative model of the response of yeast to osmotic shock. *Nat. Biotechnol.* **23** 975–982

Knott G and Kerner D 2004 *MLAB, a mathematical modeling laboratory* (Bethesda: Civilized Software Inc)

Martini S, Ricci M, Bonechi C, Trabalzini L, Santucci A and Rossi C 2004 *In vivo* ^{13}C-NMR and modelling study of metabolic yield response to ethanol stress in a wild-type strain of *Saccharomyces cerevisiae*. *FEBS Lett.* **56** 63–68

Martini S, Ricci M, Bartolini F, Bonechi C, Millucci L, Braconi D, Santucci A and Rossi C 2005 Metabolic response to exogenous ethanol in yeast: An *in vivo* NMR and mathematical modelling approach. *Biophys. Chem.* **120** 135–142

Monod J 1949 The growth of bacterial cultures. *Annu. Rev. Microbiol.* **3** 371–394

Peiter E, Fischer M, Sidaway K, Roberts SK and Sanders D 2005a Multiple RNA surveillance pathways limit aberrant expression of iron uptake mRNAs and prevent Iron toxicity in *S. cerevisiae*. *Mol. Cell* **19** 39–51

Peiter E, Fischer M, Sidaway K, Roberts SK and Sanders D 2005b The *Saccharomyces cerevisiae* Ca^{2+} channel Cch1pMid1p is essential for tolerance to cold stress and iron toxicity. *FEBS Lett.* **579** 5697–5703

Puig S, Askeland E and Thiele DJ 2005 Coordinated remodeling of cellular metabolism during iron deficiency through targeted mRNA degradation. *Cell* **120** 99–110

Ricci M, Martini S, Bonechi C, Trabalzini L, Santucci A and Rossi C 2004 Inhibition effects of ethanol on the kinetics of glucose metabolism by *S. cerevisiae*: NMR and modelling study. *Chem. Phys. Lett.* **387** 377–382

Shulman RG, Brown TR, Ugurbil K, Ogawa S, Cohen SM and den Hollander JA 1979 Cellular applications of ^{31}P and ^{13}C nuclear magnetic resonance. *Science* **205** 160–166

Shulman RG 1983 NMR spectroscopy of living cells. *Sci. Am.* **248** 86–93

Trabalzini L, Paffetti A, Scaloni A,. Talamo F, Ferro E, Coratza G, Bovalini L, Lusini P, Martelli P and Santucci A 2003 Proteomic response to physiological fermentation stresses in a wild-type wine strain of *Saccharomyces cerevisiae*. *Biochem. J.* **370** 35–46

Warwick T, Kutalik Z and Moulton V 2007 Estimating parameters for generalized mass action models using constrains propagation. *Math. Biosci.* **208** 607–620

MS received 17 June 2010; accepted 27 December 2010

*e*Publication: 14 March 2011

Corresponding editor: DURGADAS P KASBEKAR